Response of Space Shuttle Surface Insulation Panels to Acoustic Pressure

R. Vaicaitis*
Columbia University, New York, N.Y.
and
E.H. Dowell†
Princeton University, Princeton, N.J.

The free vibration characteristics and dynamic response of reusable space shuttle surface insulation panels to acoustic random pressure fields are studied. The basic analytical approach in formulating the governing equations of motion uses a Rayleigh-Ritz technique. The pressure field is modeled as a stationary Gaussian random process for which the cross-spectral density function is known empirically from experimental measurements. The response calculations are performed in both frequency and time domains. In the time domain analysis, the random noise pressures are simulated on a digital computer and the equations of motion are soived numerically in a Monte Carlo sense.

I. Introduction

THE dynamic characteristics and response of reusable space shuttle surface insulation panels to a random pressure field are studied. The current design concept for the Thermal Protection System (TPS) heatshield panels of the space shuttle consist of a relatively thick ceramic tile mounted on a soft (viscoelastic) foundation, a so-called "strain-isolator," which in turn is bonded to the primary load-carrying metal structure.[1,2] A simplified sketch of a TPS panel is shown in Fig. 1. The aeroelastic or "flutter" behavior of these panels has been investigated in Refs. 2 and 3. We will focus our attention on the free vibration characteristics of the panel and its response to acoustic excitation.

The load-carrying stiffened metallic panel is modeled as an orthotropic plate. The ceramic tile is modeled by classical thin-plate theory, while the strain isolator is taken as a linear elastic Winkler foundation.[4] The basic analytical approach in formulating the governing equations of motion uses a Rayleigh-Ritz technique. Then, by determining the relevant energies of the panel components and virtual work due to the random acoustic pressure, the necessary equations of motion are obtained by utilizing Lagrange's equation.

The pressure field is considered as a stationary Gaussian random process for which the cross-correlation function (and/or cross-spectral density) is known empirically from experimental measurements. When the Rayleigh-Ritz type solution is pursued, the cross-spectral density of the generalized random forces is required. This cross-spectral density is used directly as an input for frequency domain panel response calculations.[5,6] For the time domain approach, it is necessary to have time histories of the generalized random forces. For this purpose, the simulation techniques of random processes are utilized.[6-9] To reduce computation time, Fast Fourier Transform (FFT) techniques are introduced.[8,9]

When the frequency domain analysis is employed, the response of the panel is determined using standard methods from the theory of random processes.[10-12] By introducing systematic simplifications in this approach, useful explicit analytical formulae for panel response are constructed. These results are then compared with the results obtained by more elaborate techniques such as time domain analysis and/or finite elements.[6,13] For particular applications where the simplifying assumptions are not valid, numerical simulation of structural response time histories is used.[6,14] In this case, the panel equations of motion are solved numerically on a digital computer in a Monte Carlo sense.

The numerical results include natural modes and frequencies, and the root mean square values of the panel response to acoustic excitation. Stresses in the tiles are also calculated. Comparisons between these results and the results obtained from finite element frequency domain solutions[13] and experimental measurements[15] are included.

II. Analysis

A. Equations of Motion

The basic analytical approach in formulating the governing equations of motion of the multicomponent panel shown in Fig. 1 involves determining relevant energies and virtual work.[2,3] In Ref. 2 the main load carrying metallic substructure was analyzed as an orthotropic plate with simply supported edges, while in Ref. 3 the metallic substructure was idealized as an isotropic plate supported by discrete stiffeners and/or point spring supports. In the present study, the main metallic substructure is taken as an orthotropic plate, while the ceramic insulation tile is modeled by the classical thin-plate theory. The modeling of the strain isolator is more difficult (for a more detailed discussion see Ref. 2). For the purpose of this study, the strain isolator is represented by a linear elastic Winkler foundation. In developing the governing equations of motion for the multicomponent panel, the plate deflection w and the tile deflection w^T are expanded in terms of the trial modes:

$$w = \sum_{k_x} \sum_{k_y} b_{k_x k_y}(t)\psi_{k_x}(x)\psi_{k_y}(y) \tag{1}$$

$$w^T = \sum_{i_x} \sum_{i_y} a_{i_x}(t)\phi_{i_x}(y) \tag{2}$$

in which $b_{k_x k_y}$ and $a_{i_x i_y}$ are the generalized coordinates for the metallic plate and ceramic tile, respectively; ψ_{k_x}, ψ_{k_y} are the trial modes of the metallic plate; and ϕ_{i_x},ϕ_{i_y} are the

Presented at the AIAA/ASME/SAE 17th Structures, Structural Dynamics, and Materials Conference, King of Prussia, Pa., May 5-7, 1976 (in bound volume of Conference papers, no paper number); submitted July 18, 1977; revision received Sept. 2, 1977.

Index categories: Structural Dynamics; Aeroacoustics; Thermal Control.

*Associate Professor, Department of Civil Engineering and Engineering Mechanics. Member AIAA.

†Professor, Department of Aerospace and Mechanical Sciences. Member AIAA.

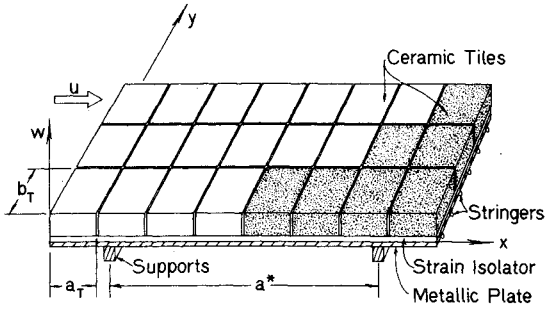

Fig. 1 Model for a surface insulation panel (space shuttle).

trial modes of the tile. The trial modes used for both metallic plate and tiles are products of free-free beam functions. After the expressions for elastic energy, kinetic energy, and virtual work are determined for the multicomponent panel shown in Fig. 1, the Rayleigh-Ritz procedure and Lagrange's equation are utilized to develop the governing equations of motion. Since this procedure is rather lengthy for the complex structure considered in this study, and the key expressions are available in Refs. 2 and 3, these equations are not included here. The result is a set of coupled linear ordinary differential equations in generalized coordinates $b_{k_x k_y}$ and $a_{i_x i_y}$. The coordinate coupling is introduced through the strain isolator.

B. Simplified Response Analysis

For the linear case considered in this paper, response calculations can be performed either in the frequency or time domain. For the time domain approach the equations of motion are solved numerically. To obtain preliminary information, we first consider a simplified response analysis in the frequency domain. The treatment follows along conventional lines, utilizing a linear structural model and stationary random process inputs whose correlation functions (and/or power spectral densities) are determined from experimental measurements.[5,10-12]

In this simplified approach, it is assumed that the mass distribution of the stiffened elastic panel can be represented by an equivalent, evenly distributed mass, and the addition of ceramic tiles merely increases the total mass of the panel. Furthermore, the tiles are assumed to be rigidly attached to the metallic substructure and to move according to the motion of the metallic substructure. Then, the panel deflection response spectral density can be written as[5]

$$S_w(\omega,x,y) = \sum_j \sum_k \psi_j(x,y)\psi_k(x,y)H_j(\omega)H_k(-\omega)S_{jk}(\omega) \tag{3}$$

in which $S_{jk}(\omega)$ is the input cross-spectral density of generalized random forces

$$S_{jk}(\omega) = \int_0^a \int_0^a \int_0^b \int_0^b S_p(\xi,\eta,\omega)\psi_j(x_1,y_1) \cdot \psi_k(x_2,y_2)\,dx_1\,dx_2\,dy_1\,dy_2 \tag{4}$$

where $S_p(\xi,\eta,\omega)$ is the cross-spectral density of the input sound pressure $p(x,y,t)$; $\xi = x_2 - x_1$; $\eta = y_2 - y_1$; and $H_j(\omega)$ is the transfer function of the structure.

$$H_j(\omega) = 1/M_j[\omega_j^2 - \omega^2 + 2i\zeta_j\omega\omega_j] \tag{5}$$

with M_j being the generalized mass

$$M_j = \int_0^a \int_0^b \psi_j^2(x,y)\,dx\,dy \tag{6}$$

and ζ_j being the modal damping coefficients.

For the cases where the random process has similar spatial correlation properties at all time delays, the input pressure cross-spectral density can be written as

$$S_p(\xi,\eta,\omega) = R_x(\xi,\omega)R_y(\eta,\omega)S(\omega) \tag{7}$$

in which R_x and R_y are the narrow band spatial correlation coefficients corresponding to the x and y coordinates, respectively, and S is the input pressure spectral density. For a convecting random process in the x direction with spatial decay, these coefficients can be expressed as

$$R_x(\xi,\omega) = \exp\left(-\frac{\omega\lambda_1}{Ua}|\xi|\right)\exp\left(i\frac{\omega\xi}{U}\right) \tag{8}$$

$$R_y(\eta,\omega) = \exp\left(-\frac{\omega\lambda_2}{Ub}|\eta|\right) \tag{9}$$

where U is the convection speed and the parameters λ_1 and λ_2 are determined experimentally.

The velocity and acceleration response spectral densities can be obtained by multiplying Eq. (3) by ω^2 and ω^4, respectively. The mean square panel deflection, velocity, and acceleration can be determined by integrating these spectral densities over the specified frequency region. It can be shown that when most of the value of these integrals comes from the vicinity of the natural frequency ω_j, and the input cross-spectral density $S_{ij}(\omega)$ is slowly varying near ω_j, the white-noise idealization can be assumed for the input spectral density.[5] Furthermore, by taking the damping in the structure to be relatively small, and the natural frequencies well separated so that intermodal coupling can be neglected, a simplified expression for the mean square deflection is obtained[5,10]:

$$\bar{w}^2(x,y) \approx \frac{\pi}{4}\sum_j \frac{\psi_j^2(x,y)}{M_j^2\omega_j^3\zeta_j}S_{jj}(\omega) \tag{10}$$

When the simplifying assumptions which lead to the analytical results presented in this section must be abandoned, numerical simulation of structural response time histories may be the method of choise.[6,15] For this purpose, the time histories of the generalized random forces are needed.

C. Generalized Random Forces

Time histories of the generalized random forces acting on the (m,n) tile shown in Fig. 1 can be determined by simulating the random pressure $P^{mn}(x,y,t)$ as a multidimensional process in the space-time domain, multiplying by the tile trial modes ϕ_{i_x} and ϕ_{i_y} and integrating over the tile dimensions. This approach for simulating generalized random forces has been described in detail in Refs. 7 and 8.

An alternative method to generate time histories of generalized random forces is to utilize the expression for the cross-spectral density of the generalized random forces, the simulation procedures of multivariate random processes, and the Fast Fourier Transform (FFT) algorithm.[7-9] Then, the generalized random force can be simulated directly as

$$Q_j^{mn}(t) = \mathrm{Re}\{(2\Delta\omega)^{1/2}\sum_{s=1}^{j}\sum_{r=1}^{N_1}|t_{js}(\omega_r)| \exp[-i(\theta_{js}(\omega_r)+\varphi_{sr})]\exp[i2\pi rk/N_1]\} \quad (k=0,1\ldots,N_1-1) \tag{11}$$

$$\theta_{js}(\omega_r) = \tan^{-1}\frac{\mathrm{Im}[t_{js}(\omega_r)]}{\mathrm{Re}[t_{js}(\omega_r)]} \tag{12}$$

where Re and Im denote the real and the imaginary part, respectively.

The elements, t_{js}, of the lower triangular matrix $[T]$ can be obtained from the cross-spectral density matrix $[S^{mn}]$ of the generalized random forces corresponding to the (m,n) tile in the following fashion:

$$[S^{mn}] = [T][T^*]' \tag{13}$$

where the asterisk indicates the complex conjugate and the prime denotes matrix transposition.

For the purpose of this study, the trial modes of individual ceramic tiles were taken to be those of a free-free beam

$$\begin{aligned}\phi_j(x) &= 1 \qquad (j=1)\\ &= \sqrt{3}(1-2x/a_T) \quad (j=2)\\ &= \exp(-\beta_j x/a_T) - (-1)^j \exp(-\beta_j(1-x/a_T))\\ &\quad + \cos(\beta_j x/a_T) - \sin(\beta_j x/a_T) \qquad (j\geq 3)\end{aligned} \tag{14}$$

where $\beta_j = 0.0, 0.0, 4.73, 7.85, \ldots$

Spatially Uniform Pressure

Consider the acoustic pressure acting on the panel to be uniformly distributed with respect to spatial coordinates (x,y) and varying randomly in time. For this case, due to the orthogonality principle, only the first tile mode contributes to the generalized random force. Then, the cross-spectral density of the generalized random force reduces to

$$\begin{aligned}S_{jk}^{mn}(\omega) &= a_T^2 b_T^2 S_p^{mn}(\omega) \quad (j=k=1)\\ &= 0 \quad \text{otherwise}\end{aligned} \tag{15}$$

and the time history of the generalized random force can be simulated from

$$\begin{aligned}Q_j^{mn}(t) &= a_T b_T \sqrt{2} \sum_{i=1}^{N_I} [S_p^{mn}(\omega_i)\Delta\omega]^{1/2} \cos[\omega_i t + \varphi_i]\\ &\qquad\qquad (\text{for } j=1)\\ &= 0 \quad \text{otherwise}\end{aligned} \tag{16}$$

in which S_p^{mn} is the input pressure spectral density for the (m,n) tile.

Convected Random Pressure

Consider the acoustic pressure to be uniform in the spanwise direction and convected as random plane waves in the streamwise direction. The cross-spectral density in this case can be expressed as[16]

$$S_p^{mn}(\xi,\omega) = S_p^{mn}(\omega)\ \exp(i\omega\xi/U) \tag{17}$$

in which U is the convection speed of the random plane waves. From Eqs. (4), (14), and (17), it can be shown that

$$S_{jk}^{mn}(\omega) = S_p^{mn}(\omega) b_T^2 a_T^2 [J_{jk}(\omega) + iK_{jk}(\omega)] \tag{18}$$

in which

$$J_{jk}(\omega) = I_c^j I_c^k + I_s^j I_s^k \tag{19a}$$

$$K_{jk}(\omega) = I_s^j I_c^k - I_c^j I_s^k \tag{19b}$$

$$I_{c,s}^j = \{\lambda_{c,s}'' \phi_j' |_0^1 - \lambda_{c,s}''' \phi_j |_0^1\} / (\beta_j^4 - \alpha^4) \tag{20a}$$

$$\lambda_c'' = -\alpha^2 \cos(\alpha x/a_T) \qquad \lambda_s''' = \alpha^3 \sin(\alpha x/a_T) \tag{20b}$$

$$\lambda_s'' = -\alpha^2 \sin(\alpha x/a_T) \qquad \lambda_s''' = -\alpha^3 \cos(\alpha x/a_T) \tag{20c}$$

with $\alpha = -a_T/U$ and the prime indicating a derivative $(\equiv \mathrm{d}/\mathrm{d}(x/a_T))$. It should be noted that for

mode j symmetric, mode k antisymmetric,

$$J_{jk} = 0$$

mode j symmetric, mode k symmetric,

$$K_{jk} = 0$$

mode j antisymmetric, mode k antisymmetric,

$$K_{jk} = 0$$

and

$$J_{jk} = J_{kj} \qquad K_{jk} = -K_{kj}$$

Then, the time histories of the generalized random forces due to convected pressure can be generated from Eqs. (11) and (18).

When the spatial correlation coefficients are of the form given in Eqs. (8) and (9), the procedure for determining the cross-spectral densities or time histories of the generalized random forces is similar to that described in this section. However, the expressions are rather lengthy and they are not included in this paper.

D. Response Simulation

For the time domain approach, the governing differential equations of motion[2,3] are combined with the time histories of the generalized random forces given in Eq. (11). Utilizing a step-by-step temporal numerical integration and the modal expansion for panel and tile deflections presented in Eqs. (1) and (2), time histories of $w(x,y,t)$ and $w^T(x,y,t)$ are determined. By assuming the response process to be ergodic, the mean square response can be obtained using the temporal average. For example, the mean square response of the metallic panel deflections is

$$\bar{w}^2(x,y) = \frac{1}{T_0}\int_0^{T_0} (w(t,x,y))^2 \mathrm{d}t \tag{21}$$

in which T_0 is the sample duration. The panel deflection response spectral density S_w can be calculated utilizing the Fast Fourier Transform (FFT) algorithm on the response history $w(x,y,t)$.[8,9]

The stress response in the metallic plate and the supporting stringers can be determined from the information on the curvature corresponding to deflection $w(x,y,t)$. For example, the maximum stress in the stringer can be estimated from

$$\sigma_{sT} = E_M d^* \frac{\partial^2 w}{\partial x^2} \tag{22}$$

where d^* is the maximum distance between the centroid of the cross section and outer edge of the stringer, and E_M is the elastic modulus of the stringer. Similarly, the maximum bending stress in the tile is estimated by

$$\sigma_{\text{tile}} = E_T \frac{t_T}{2} \frac{\partial^2 w^T}{\partial x^2} \tag{23}$$

where t_T and E_T are the thickness and the elastic modulus of the tile, respectively. The normal stress in the tile can be calculated from the following formula

$$\sigma_{\text{tile}}^n = (E_{z_1}/t_1)(w - w^T) \tag{24}$$

Table 1 Physical parameters for RSI panels

Tile	
E_T, psi	$24 \pm \frac{5}{10} \times 10^3$
t_T, in.	1, 1.6, 2.3
ρ_T, lb/ft^3	9
ν_T	.179
a_T, in.	6
b_T, in.	6
Isolator	
E_{z_I}, psi	15 ± 10
t_I, in.	.16
Metallic	
E_M, psi	10.5×10^6
ν_M	.33
ρ_M, lb/in.^{3}	1
D_x, lb-in.	220,000
D_y, lb-in.	31
D_{xy}, lb-in.	9812 or 3300
D_I, lb-in.	9
$m_M = \rho_M (t_M)_{\text{avg}}$, lb/in^2	.0083
Neutral axis location, in. (from top of skin)	.43
a_M, in.	54 or 48
b_M, in.	18

Note: Metallic plate is assumed pinned on line supports 37 in. apart. All outer edges are free. The structural damping without tiles is in the range $\zeta = .005 - .01$ (Ref. 16); with tiles it is expected to be somewhat higher. The amount of acoustic or aerodynamic damping is unknown.

in which E_{z_I} and t_I are the elastic modulus and the thickness of the strain isolator, respectively.

III. Numerical Results

A. Natural Modes and Frequencies

The physical parameters of the structural configuration studied are shown in Table 1. The principal parameter which varied is t_T. There is considerable uncertainty in the isolator modulus E_{z_I}; however, calculations have indicated that the lower natural frequencies were not sensitive to this parameter. This is not necessarily true for stress response due to acoustic loads however, nor for natural frequencies with other combinations of the remaining parameters.

It was found necessary to modify empirically the metallic plate twisting stiffness D_{xy} to give better agreement with the experiment. The orthotropic plate stiffnesses were calculated by conventional methods as described in the Appendix. D_{xy} was calculated using Bredt's formula for torsion of a tube. The theoretical value, 9812 lb-in., was found to be approximately three times higher than the empirical value which gave the best agreement with experiment, 3300 lb-in. To verify that the difficulty was in estimating D_{xy} per se rather than in using an orthotropic plate model, a separate calculation was made in which the stiffeners were treated as discrete beam-torsion tubes attached to an isotropic plate (skin). The results were virtually identical to the orthotropic plate model. Also see Ref. 13 on this point.

Metallic Plate Only

In Table 2 natural frequencies are shown as determined from experiment,[15] from finite element analysis,[13] and from the present theory. The latter results differ by the panel length, 54 in. or 48 in., and D_{xy}, 9812 lb-in. or 3300 lb-in. As mentioned previously, $D_{xy} = 3300$ lb-in. gives the best fit to the experimental data. The actual panel length was 54 in; however, a length of 48 in. was also considered since that length was used for the case with tiles added (see discussion below). The mode identification numbers have the following meaning.

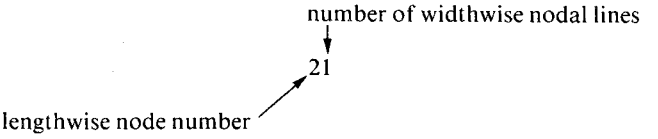

Metallic Plate with Isolator and Tiles

Natural frequencies are given in Table 3. All these results are for a total metallic plate length of 48 in. The actual length is 54 in.; however, 3 in. on each end is not covered with tiles and is not accounted for in the present analysis. A total of $8 \times 3 = 24$ 6×6 in. tiles cover the 48×18 in. metallic plate. The results for no tiles are also shown for reference.

For the first lengthwise modes, a simple mass scaling gives rather accurate results; i.e., if one simply adds the tile mass to that of the metallic plate, one obtains the results shown in brackets in Table 3. The results for the higher chordwise or lengthwise modes are less satisfactory using mass scaling.

In Table 3 there is a rapid increase in frequency from the 13th mode to the 14th mode. This is probably related to the number of tiles (and associated nodes) in the widthwise direction, i.e., three. In most of the present calculations, each tile was allowed four degrees of freedom, two in the lengthwise and two in the widthwise direction. The metallic panel was allowed six lengthwise and eight widthwise degrees of freedom. Hence the higher lengthwise and widthwise modes shown may be somewhat less accurately determined than the lower modes. A few calculations with additional degrees of freedom for tiles and metallic panel indicated good convergence however.

Discussion

It should be emphasized that the present results are not necessarily typical of all space shuttle RSI TPS structure. For other combinations of parameters, the effect of the tiles may be to raise the natural frequencies above those for the metallic panel alone. Two key parameters, based upon the present results and those of Ref. 3, as well as a little physical intuition, appear to be

$$D_M/D_T$$

and

$$\frac{D_M}{a_M^4} \Big/ \frac{D_T}{a_T^4}$$

In the present case

$$D_M/D_T = 106.5 - 8.8$$

and

$$\frac{D_M}{a_M^4} \Big/ \frac{D_T}{a_T^4} = 0.026 \rightarrow 0.0021$$

$D_M/D_T \gg 1$ insures that the stiffness of the tile will have little effect. On the other hand

$$\frac{D_M}{a_M^4} \Big/ \frac{D_T}{a_T^4} \gg 1$$

means the individual tiles behave as rigid bodies. Note that

$$\frac{D_M}{b_M^4} \Big/ \frac{D_T}{b_T^4} = 1.3 \rightarrow 0.11$$

Table 2 Natural frequencies for metallic panel

	Experiment[15] 54 in.		Theory 54 in.	Theory 54 in.	Theory 48 in.	Finite element[13] 48 in.	
Mode	Vibration test	Acoustic chamber test	$D_{xy}=9812$	$D_{xy}=3300$	$D_{xy}=3300$	Orthotropic	Discrete stringer
10	97-113	103	107	107	114	107	107
11	130	131	168	132	135	135	133
12	187	187	268	185	185	186	174
13	250	257	327	247	246	205	224
14	319	320	486	316	317		313
15	388	380	599	388	392		381
16	434	436		483	489		412
20	264		373	327	425		
21	469		401	354	448		
22	512		466	425	512		
23	562				602		
24	633						
25	702						

Table 3 Natural frequencies of metallic panel with tiles

	No tiles		$t_T=1$ in.	$t_T=1.6$ in.	$t_T=2.3$ in.		Finite element,[13] $t_T=2.3$ in	
Mode	Theory (48 in. length)	Experiment	Theory	Theory	Theory	Experiment	Tile density 9 lb/ft^3	Tile density 11 lb/ft^3
10	114	97-113	91 [89][a]	80 [81]	72 [70]	67	77	72
11	135	130	109	95	86	103	99	84
12	185	187	150	132	117	122	107	100
13	246	250	195	170	150	141	145	136
14	317	319	290	245	206	231	183	171
15	392	388	357	293	243			
16	489	434						
20	425	264	290	241	206	193		
21	448	469	302	249	212	204		
22	512	512	329	268	227	217		
23	602	562	358	288	242			

[a] Results in brackets, [...], were obtained by simple mass scaling.

Hence, bending of the tiles in the widthwise direction may be more important than in the lengthwise direction when bending of the metallic panel occurs. Recall the earlier discussion on this point. Calculations for the 2.3 in tiles which allowed for tile bending in the widthwise direction showed little change from the rigid tile results.

As mentioned previously, the isolator modulus is not accurately known. Fortunately, calculations indicate the lower natural frequencies are not sensitive to moderate changes in this parameter.

B. Structural Response to Random Pressure Loading

1. Simplified Analysis

As an example, consider an orthotropic panel (with and without tiles) free at the edges $y=0$, b and simply supported along the line supports (Fig. 1). The physical data for this panel are given in Table 1. We shall assume initially that this panel is loaded by acoustic random pressure for which the power-spectral density scaled from Saturn V liftoff data is shown in Fig. 2. This pressure spectral density is taken from Ref. 17.

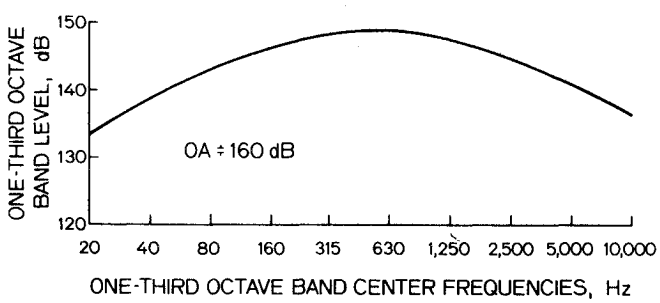

Fig. 2 Liftoff acoustic noise spectra for orbiter payload bay doors based on Saturn V scale model.

Uniform Pressure—Consider the acoustic noise pressure to be fully correlated in space over the panel surface. The aluminum panel has the following properties: $E_M=10.5\times10^6$ psi, $a=48$ in., $a^*=37$ in. (distance between the line supports), $b=18$ in., $\rho_M=0.1$ lb/in.^{3}, $(t_M)_{avg}=0.083$ in., $d^*=0.972$ in., $m_M=0.0083/386$ (lb-sec^2)/(in.^{3}). The natural frequencies for the untiled panel are given in Table 2. Assume for simplicity that the streamwise panel vibration mode can be approximated here by

$$\psi_m(x)=\sin(m\pi x/a^*) \tag{25}$$

and ignore the portion of the panel beyond the line supports. From Eqs. (4), (14), and (25), the cross-spectral densities of generalized random forces are

$$S_{mn}(\omega)=S(\omega)(a^*/m\pi)^2b^2[(-1)^m-1]^2 \quad (n=1)$$
$$=0 \quad \text{otherwise} \tag{26}$$

From Eqs. (10), (22), (26) and Fig. 2, the root-mean-square panel deflections, stringer stresses and stringer strains can be calculated. These results are presented in Table 4 at $x=a^*/2$ and $y=b/2$.

Table 4 Root-mean-square response to uniform random pressure, liftoff environment, frequency domain analysis

Tile thickness t_T, in.	Damping c/c_{cr}	Deflection $\bar{w}$, in. Present analysis	Deflection $\bar{w}$, in. Finite element Ref. 13	Stringer stress σ_{ST}, psi Present analysis	Stringer stress σ_{ST}, psi Finite element Ref. 13	Stringer strain $\epsilon_{ST}\times 10^4$ in./in. Present analysis
	0.005	0.143	0.133	10,409	9,504	9.91
0	0.01	0.101	0.094	7,360	6,718	7.01
(no tiles)	0.02	0.071	0.067	5,204	4,752	4.96
	0.005	0.122	0.096	8,943	6,912	8.52
1.0	0.01	0.086	0.068	6,324	4,882	6.02
	0.02	0.062	0.048	4,471	3,456	4.26
	0.005	0.116	0.096	8,811	7,093	8.39
1.6	0.01	0.082	0.067	6,230	5,011	5.93
	0.02	0.059	0.048	4,405	3,547	4.20
	0.005	0.104	0.094	7,703	7,214	7.34
2.3	0.01	0.074	0.067	5,447	5,098	5.19
	0.02	0.052	0.047	3,852	3,607	3.67

Addition of Tiles—With the 2.3-in. tiles attached to the metallic plate, the mass of the metallic plate and tile is

$$m_p = (m_M + 0.012/386) = 0.0203 \text{ lb-s}^2/\text{in}^3 \tag{27}$$

and the natural frequencies are given in Table 3. The calculated results with the ceramic tiles added are given in Table 4. Results from finite element analysis given in Ref. 13 are included in Table 4. These values, obtained for somewhat different random pressure inputs, were scaled to the inputs considered in this study.

Convected Random Pressure—We shall now consider the input pressure to be convected in the streamwise direction over the panel surface and characterized by the cross-spectral density of the following form:

$$S_p(\xi,\omega) = S(\omega)\cos(\omega\xi/U) \tag{28}$$

From Eqs. (4), (14), (25), and (28), the cross-spectral densities of the generalized forces are

$$S_{mn}(\omega) = S(\omega)\frac{(m\pi/a^*)^2\,[1-(-1)^m\cos(\omega a/U)]^2 b^2}{[(m\pi/a^*)^2-\omega/U^2]^2}(n=1)$$

$$=0 \quad \text{otherwise} \tag{29}$$

When U is equal to the speed of sound at sea level, i.e., $U=13{,}210$ in./s, the numerical results corresponding to convected noise pressure are presented in Table 5.

As can be seen, *in this case*, the convection of the random pressures field has a modest effect.

Partially Coherent Pressure—When the input pressure acting on the panel surface varies randomly in space, the effects of spatial correlations need to be included. This can be accomplished by using Eq. (7) for which the correlation coefficients are given in Eqs. (8) and (9). Limiting the analysis to the first spanwise mode ($n=1$ in Eq. (14)) and using Eqs. (4), (7), (8), and (9), it can be shown that

$$S_{ml} = S(\omega)\,\frac{4a^{*2}b^2}{(\omega\lambda_2/U)^2}\,[(\omega\lambda_2/U)+e^{-\omega\lambda_2/U}-1]$$

$$\times\frac{[(m\pi)^2(1-(-1)^m e^{-q})+q(q^2+(m\pi)^2)/2]}{[q^2+(m\pi)^2]^2} \tag{30}$$

where

$$q=\frac{\omega\lambda_1}{U}+\frac{i\omega a^*}{U} \tag{31}$$

Table 5 Root-mean-square response to convected (no spatial decay) random pressure, liftoff environment, frequency domain analysis

Tile thickness t_T, in.	Damping c/c_{cr}	Deflection $\bar{w}$, in.	Stringer stress σ_{ST}, psi	Stringer strain $\epsilon_{ST}\times 10^4$, in./in.
0	0.005	0.130	9,493	9.04
(no tiles)	0.01	0.091	6,712	6.39
	0.02	0.065	4,746	4.52
	0.005	0.115	8,415	8.02
1.0	0.01	0.081	5,951	5.66
	0.02	0.058	4,207	4.01
	0.005	0.111	8,406	8.00
1.6	0.01	0.078	5,943	5.66
	0.02	0.056	4,202	4.01
	0.005	0.100	7,395	7.05
2.3	0.01	0.071	5,229	4.98
	0.02	0.050	3,698	3.52

Utilizing these expressions, the root-mean-square response of the panel to partially coherent input pressure can be calculated. These results are shown in Table 6. The correlation parameters λ_1 and λ_2 used for these calculations correspond to typical values found in a turbulent boundary layer.

2. Simulation Analysis

Generalized random forces representative of those due to sound pressure near the base of the orbiter at shuttle liftoff were generated in the time domain from Eq. (11). It was assumed that the input pressure is convected as random plane waves at the fluid speed of sound for which the input cross-spectral density of the generalized random forces is given in Eq. (29). When the ceramic tiles were attached to the panel, it was assumed that each tile had an identical input pressure-spectral density, i.e., $S^{mn}(\omega)=S(\omega)$. Numerical computations are limited to three streamwise modes and one spanwise mode (Eq. (14)). To simulate the elastic supports in the spanwise direction (Fig. 1), twenty points, at $x=5.5$ in. and $x=42.5$ in. across the panel, were chosen. At each point an elastic translation spring with stiffness of 1×10^4 lb/in. were assumed to be attached. Simulation of generalized random forces was accomplished utilizing the following data: $U=13{,}210$ in./s, $N_l=512$, $\omega_u=2\pi\times1000$ rad/s. The physical data for the panel are given in Table 1. It was assumed that the critical damping ratio in each mode is the same. Utilizing these time histories and panel equations of

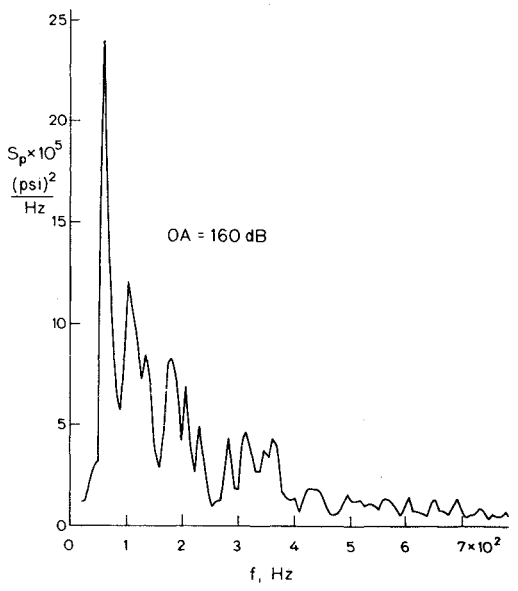

Fig. 3 Experimental pressure spectral density in acoustic test chamber (160 dB OA).

motion,[2,3] panel response in the time domain was determined. The root-mean-square response corresponding to panel deflection and stress and strain in the stringer, at the location $\bar{x}=x/a=0.5$ and $\bar{y}=y/b=0.5$ is presented in Table 7 for a combination of several tile thicknesses, damping coefficients, and the two input spectral densities shown in Figs. 2 and 3. The experimental input pressure-spectral density shown in Fig. 3 was obtained in the acoustic chamber test facility at Langley Research Center (Ref. 15). The experimental stringer strains in this test facility were obtained for 150 dB and 157 dB OA inputs. The stringer strains corresponding to 160 dB OA inputs shown in Table 7 were scaled from these measurements. The normal stresses in each tile along the centerline of the panel are shown in Fig. 4. These latter results were obtained from Eq. (24) using the input spectral density shown in Fig. 2.

IV. Conclusions

Free vibration results show good agreement with results obtained by the finite element method[13] and by the experimental measurements. The agreement between time domain and simplified fretcdomain analysis is fairly good (cf. Tables 5 and 7), and for preliminary response calculations the simplified spectral density approach can be used. However,

Table 6 Root-mean-square response to partially coherent random pressure, liftoff environment, frequency domain analysis

Tile thickness t_T, in.	Damping c/c_{cr}	Deflection $\bar{w}$, in. $\lambda_1/a^*=0.5$ $\lambda_2/b=1.0$	Deflection $\bar{w}$, in. $\lambda_1/a^*=1.0$ $\lambda_2/b=2.0$	Stringer stress σ_{ST}, psi $\lambda_1/a^*=0.5$ $\lambda_2/b=1.0$	Stringer stress σ_{ST}, psi $\lambda_1/a^*=1.0$ $\lambda_2/b=2.0$	Stringer strain $\epsilon_{ST}\times10^4$ in./in. $\lambda_1/a^*=0.5$ $\lambda_2/b=1.0$	Stringer strain $\epsilon_{ST}\times10^4$ in./in. $\lambda_1/a^*=1.0$ $\lambda_2/b=2.0$
	0.005	0.099	0.082	7,338	5,899	7.01	5.63
0	0.01	0.071	0.058	5,204	4,183	4.91	3.99
(no tiles)	0.02	0.050	0.041	3,691	2,976	3.52	2.83
	0.005	0.091	0.078	6,841	5,690	6.50	5.41
1.0	0.01	0.065	0.055	4,851	4,035	4.61	3.84
	0.02	0.046	0.039	3,441	2,862	3.27	2.72
	0.005	0.095	0.079	6,984	5,910	6.66	5.63
1.6	0.01	0.067	0.056	4,953	4,192	4.72	3.99
	0.02	0.048	0.040	3,513	2,973	3.35	2.83
	0.005	0.094	0.078	6,879	5,899	6.54	5.61
2.3	0.01	0.066	0.055	4,879	4,183	4.62	3.98
	0.02	0.047	0.039	3,460	2,967	3.29	2.82

Table 7 Root-mean-square response to convected (no spatial decay) random pressure, time domain analysis

Tile thickness t_T, in.	Damping c/c_{cr}	Deflection $\bar{w}$, in. Input liftoff environment Fig. 2	Deflection $\bar{w}$, in. Input acoustic chamber Fig. 4	Stringer stress σ_{ST}, psi Input liftoff Fig. 2	Stringer stress σ_{ST}, psi Input acoustic chamber Fig. 4	Stringer strain $\epsilon_{ST}\times10^4$, in./in. Input liftoff Fig. 2	Stringer strain $\epsilon_{ST}\times10^4$, in./in. Input acoustic chamber Fig. 4	Stringer strain $\epsilon_{ST}\times10^4$, in./in. Experimentally measured[16] in acoustic chamber
0	0.005	0.134	0.112	9,830	8,250	9.32	7.85	
(no tiles)	0.01	0.095	0.079	7,055	5,860	6.63	5.56	2.54
	0.02	0.068	0.056	4,996	4,140	4.76	3.92	
	0.005	0.117	0.103	8,373	7,410	8.14	6.95	
1.0	0.01	0.083	0.072	5,921	5,220	5.72	4.90	No data
	0.02	0.058	0.051	4,196	3,743	4.05	3.49	available
	0.005	0.103	0.105	7,910	7,320	7.56	6.90	
1.6	0.01	0.075	0.071	5,597	5,180	5.37	4.86	No data
	0.02	0.054	0.051	3,960	3,687	3.75	3.45	available
	0.005	0.081	0.079	6,060	5,960	5.81	5.40	
2.3	0.01	0.049	0.056	3,747	4,210	3.67	3.82	1.50
	0.02	0.036	0.040	2,707	2,894	2.58	2.70	

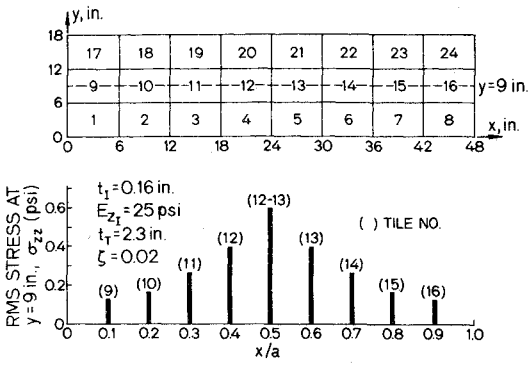

Fig. 4 Normal stresses in the tiles; liftoff environment.

the simplified frequency domain approach using a few structural modes tends to overestimate the response by about 10% when compared to the finite element solution.[13] In modeling the random pressure input loading, spatial decay is more significant than convection for the conditions studied.

The stringer strains measured in the acoustic chamber were about one-half of those calculated. A principal reason for this difference is the spatial nonuniformity in the experimental input pressure distribution as well as the large pressure power spectral density variations in a very narrow frequency band. In addition there is the usual uncertainty in the damping in the structure.

Theoretically determined responses for liftoff conditions and the acoustic chamber tests were similar, indicating a good simulation was achieved experimentally except for the narrow band frequency variations in the acoustic chamber pressure power spectral density previously mentioned.

Appendix: Calculation of Orthotropic Plate Constants

$A = \Sigma A_i$ A_i = cross-sectional area of each element

I_0 = area moment of skin alone

$\bar{z} \equiv \Sigma A_i z_i / A$ $\bar{z}$ = neutral axis location

z_i = vertical center of each element

$I_{NA} = [I_0 + \Sigma_i A_i z_i^2 - A\bar{z}^2]$ I_{NA} = area moment about neutral axis

$D_x = E_M I_{NA} / d$

d = spacing between stiffeners

$D_y = E_M t_M^3 / 12(1 - \nu_M^2)$

$D_{xy} = G/d[A^2{}_{\text{eff}} / \Sigma l_i t_i]$

A_{eff} = area enclosed by stiffeners

l_i = length of each element

t_i = thickness of each element

$D_1 = \nu_M D_y$

The stiffeners are constructed from several straight line elements each of which has a certain z_i, t_i, l_i and A_i. A_{eff} is the "torque tube" area.

Acknowledgment

This work was supported by NASA Grants NSG-1059 and NGR 31-001-146, Langley Research Center.

References

[1] Bohon, H.L., "Thermal Protection Systems for Space Shuttle," *Development Status of Reusable Non-Metallic Thermal Protection,"* edited by D. Greenshields, G. Strouhal, D. Tilliam, and J. Pawloski, TMX-2273, April 1971.

[2] Dowell, E.H., "Vibration and Flutter Analysis of Reusable Surface Insulation Panels, *Journal of Spacecraft and Rockets,* Vol. 12, Jan. 1975, pp. 44-50.

[3] Dowell, E.H., "Theoretical Vibration and Flutter Studies of Point Supported Panels," *Journal of Spacecraft and Rockets,* Vol. 10, June 1973, pp. 380-395.

[4] Dowell, E.H., "Dynamic Analysis of An Elastic Plate on A Thin, Elastic Foundation," *Journal of Sound and Vibration,* Vol. 35, Aug. 1974, pp. 343-360.

[5] Dowell, E.H. and Vaicaitis, R., "A Primer for Structural Response to Random Pressure Fluctuations," Princeton University, AMS Rept. No. 1220, April 1975.

[6] Vaicaitis, R., "Random Input and Response Study of Multicompoent Panels," Dept. of Civil Engineering and Engineering Mechanics, Columbia University, TR-1, July 1975; prepared for NASA under NSG-1059.

[7] Shinozuka, M. and Jan, C.M., "Digital Simulation of Random Processes and its Applications," *Journal of Sound and Vibration,* Vol. 25, Nov. 1972, pp. 111-128.

[8] Vaicaitis, R., "Generalized Random Forces for Rectangular Panels," *AIAA Journal,* Vol. 11, July 1973, pp. 984-988.

[9] Shinozuka, M., "Digital Simulation of Random Processes in Engineering Mechanics with the Aid of FFT Technique in Stochastic Problems in Mechanics," edited by S.T. Ariaratnam and H.H.E. Liepholz, University of Waterloo Press, 1974, pp. 277-286.

[10] Miles, J.W., "On Structural Fatigue Under Random Loading," *Journal of Aeronautical Sciences,* Vol. 21, Nov. 1954, pp. 753-762.

[11] Powell, A., *Random Vibration,* edited by S.H. Crandall, Technology Press, Cambridge, Mass., 1958, Chap. 8.

[12] Lin, Y.K., *Probabilistic Theory of Structural Dynamics,* McGraw-Hill, New York, 1967.

[13] Ojalvo, I.U. and Ogilvie, P.L., "Modal Analysis and Dynamic Stresses for Acoustically Excited Shuttle Insulation Tiles," NASA CR-144958, Aug. 1975; also *Proceedings AIAA/ASME/SAE 17th Structures, Structural Dynamics, and Materials Conference,* King of Prussia, Pa., May 1976, pp. 273-281.

[14] Vaicaitis, R., Dowell, E.H., and Ventres, C.S., "Nonlinear Panel Response by a Monte Carlo Approach," *AIAA Journal,* Vol. 12, May 1974, pp. 685-691.

[16] Mercer, C.A., "Response of Multi-Supported Beam to a Random Pressure Field," *Journal of Sound and Vibration,* Vol. 2, July 1965, pp. 293-306.

[15] Rucker, C.E. and Mixson, J.S., "Vibro-Acoustic Testing of Space Shuttle Thermal Protection System Panels," *Proceedings AIAA/ASME/SAE 17th Structures, Structural Dynamics, and Materials Conference,* King of Prussia, Pa., May 1976, pp. 248-256; also personal communication with Carl Rucker.

[17] "An Interim Report on Shuttle Orbiter Vibroacoustics," Vibration and Acoustic Unit, Space Division, Rockwell International Corporation," presented at Shock and Vibration Symposium, Albuquerque, N.Mex., Oct. 19-21, 1976.